Pergamon

Int. J. Heat Mass Transfer. Vol. 39, No. 9, pp. 1847–1857, 1996

0017-9310/96 $15.00+0.00

0017-9310(95)00274-X

Thermal stability of horizontally superposed porous and fluid layers in a rotating system

JONG JHY JOU

Department of Applied Mathematics, Feng Chia University, Taichung, Taiwan 40724, Republic of China

and

KUANG YUAN KUNG and CHENG HSING HSU

Department of Mechanical Engineering, Chung Yung University, Chung Li, Taiwan 32054, Republic of China

(*Received* 14 *December* 1994 *and in final form* 21 *July* 1995)

Abstract—The onset of thermal stabilities of the horizontally superposed systems of fluid and porous layers, in a rotating coordinate, is investigated. Boussinesq's approximation, local volume average technique and Darcy's law are employed and the slipping interface is assumed. The top and bottom boundaries of the system are assumed rigid and isothermal. A Sturm–Liouville's problem is derived and solved numerically. The critical Rayleigh number R_c or R_{mc} and wavenumber a_c or a_{mc} are obtained for various values of depth ratio $\hat{d}$, thermal conductivity ratio k/k_m, permeability K, proportionality constant in the slip condition $\tilde{\alpha}$ and Taylor number Ta. The sole effect of rotation is stabilizing. The previous results with $Ta = 0$, using different methods, are compared very well.

INTRODUCTION

The thermal stability of the horizontally superposed systems of porous and fluid layers has been previously studied [1–5]. The present paper, including the rotation effect, is accomplished, using a different but more systematic mathematical and numerical approach, which can be easily modified to solve generalized problems.

The horizontally superposed systems of porous and fluid layers, between which heat and mass transfers occur through the interface, are related to many natural phenomena and industrial applications. The water layer of pond, lake or ocean sits on a layer of mud, sediment, sand, stone or rock. The underground water or petroleum may be stored inside or between porous layers of rock. Geophysically, there is, lying between the solid inner core and liquid outer core of the earth, a freezing porous zone which mechanism may account for the occurrence and variation of the geomagnetic field [6]. Metallurgically, a similar mechanism may profoundly affect the quality of metal alloy [7]. Furthermore, nuclear reactor, water cooling system and oil storing tank are all good examples in application.

The local volume average technique [8] is applied to describe the global effect of the porous layer. The momentum equation, governing the porous layer, may include the frictional drag of porous boundary effects, $-(\mu/K)\mathbf{u}_m$, the form drag of inertial effect, $-\rho F(\delta^{3/2}/K^{1/2})(\mathbf{u}_m \cdot \mathbf{u}_m)\mathbf{I}$, and the viscous shear term, $\mu\nabla^2\mathbf{u}_m$ [1, 3, 5, 9, 10]. There are two approaches for describing the boundary conditions at the interface between the fluid and porous layers. The Brinkman's equation of non-slip condition suggests that velocity and shear stress are continuous at the interface [9, 11], while the slip conditions at the interface assume the forms [1, 3–5, 12, 13]:

$$\frac{\partial u}{\partial z} = \frac{\tilde{\alpha}}{\sqrt{K}}(u - u_m)$$

$$\frac{\partial v}{\partial z} = \frac{\tilde{\alpha}}{\sqrt{K}}(v - v_m).$$

All steady slow motions in a rotating inviscid fluid are necessarily two-dimensional (2D) and the Taylor–Proudmann theorem predicts that the sole effect of rotation is stationarily stabilizing [14].

The onset of thermal stabilities of the horizontally superposed systems of the fluid and porous layers, in a rotating system, is investigated. Three systems are shown in Fig. 1, case (a) a porous layer sandwiched between two fluid layers, case (b) a fluid layer overlying a porous medium and case (c) a fluid layer sandwiched between two porous layers. Boussinesq's approximation, local volume average technique and Darcy's law are employed for the momentum equation of the porous layer. The boundary conditions, at the interface between the fluid and porous layers, are assumed slipping and the top and bottom boundaries are rigid and isothermal.

NOMENCLATURE

- a wavenumber in the fluid layer
- a_m wavenumber in the porous layer
- C thermal capacity of the fluid
- C_s thermal capacity of the solid
- d depth of the fluid layer
- d_m depth of the porous layer
- $\hat{d}$ depth ratio, d_m/d
- D differential operator
- D_f thermal diffusivity of the fluid layer
- D_{fm} thermal diffusivity of the porous layer, α_e/ρ_e
- g gravity
- k thermal conductivity of the fluid layer
- k_m thermal conductivity of the porous layer
- K permeability
- Pr Prandtl number for the fluid layer, ν/D_f
- Pr_m Prandtl number for the porous layer, ν/D_{fm}
- R Rayleigh number for the fluid layer, $g\alpha\beta d^4/\nu D_f$
- R_m Rayleigh number for the porous layer, $g\alpha\beta_m d_m^4/\nu D_{fm}$
- t dimensionless time
- t' time
- Ta Taylor number for the fluid layer, $4\Omega^2 d^4/\nu^2$
- Ta_m Taylor number for the porous layer, $4\Omega^2 d_m^4/\nu^2$
- T_l temperature at the bottom boundary
- T_u temperature at the top boundary
- $\mathbf{u}$ velocity vector in the fluid layer, (u, v, w)
- $\mathbf{u}_m$ velocity vector in the porous layer, (u_m, v_m, w_m)
- x, y, z dimensionless Cartesian coordinates
- x', y', z' Cartesian coordinates.

Greek symbols

- α thermal expansion coefficient
- $\tilde{\alpha}$ constant of proportionality in the slip condition
- α_e effective thermal diffusivity, $[k\delta+k_s(1-\delta)]/[\rho C\delta+\rho_s C_s(1-\delta)]$
- β $k_m(T_l-T_u)/(k_m d+kd_m)$
- β_m $k(T_l-T_u)/(k_m d+kd_m)$
- ε_t $(k/k_m)\hat{d}$
- $\bar{\varepsilon}_t$ $(D_f/D_{fm})\hat{d}$
- ζ vorticity in the fluid layer
- ζ_m vorticity in the porous layer
- θ perturbed temperature of the fluid layer
- θ_m perturbed temperature of the porous layer
- μ dynamic viscosity
- ν kinematic viscosity
- ρ_e effective thermal capacity, $\rho C\delta/[\rho C\delta+\rho_s C_s(1-\delta)]$
- Ω frequency of rotation
- ω, ω_m frequency.

Superscript

- $'$ perturbation quantity.

Subscripts

- m porous layer
- c critical value.

PHYSICAL FORMULATION

A set of scales (d, d, d^2/D_f, D_f/d^2, D_f/d, βd, d_m, d_m, d_m^2/D_{fm}, D_{fm}/d_m^2, D_{fm}/d_m, $\beta_m d_m$, d_m^2) for lengths x' and y', time t', vertical vorticity ζ', velocity $\mathbf{u}'$, and perturbed temperature θ' of the fluid layer and for lengths x'_m and y'_m, time t'_m, vertical vorticity ζ'_m, velocity $\mathbf{u}'_m$, perturbed temperature θ'_m and permeability K of the porous layer. Also, z and z_m are defined as $z = (z'-d_m)/d$ and $z_m = z'/d_m$ for cases (a) and (b) and $z = z'/d$ and $z_m = (z'-d)/d_m$, for case (c).

We may seek solutions in terms of normal modes for w', θ', ζ', w'_m, θ'_m and ζ'_m,

$$[w', \theta', \zeta'] = [w(z), \theta(z), \zeta(z)] \cdot \exp[\omega t + i(k_1 x + k_2 y)]$$

$$[w'_m, \theta'_m, \zeta'_m] = [w_m(z_m), \theta_m(z_m), \zeta_m(z_m)] \cdot \exp[\omega_m t_m + i(k_{1m} x_m + k_{2m} y_m)]$$

where $a = \sqrt{(k_1^2+k_2^2)}$ and $a_m = \sqrt{(k_{1m}^2+k_{2m}^2)}$ are wavenumbers. The linearized governing equations in dimensionless forms, for the fluid layer, are [1, 2, 15]

$$\nabla \cdot \mathbf{u} = 0 \tag{1}$$

$$\left(D^2 - a^2 - \frac{\omega}{Pr}\right)\zeta + \sqrt{(Ta)}Dw = 0 \tag{2}$$

$$(D^2-a^2)\left(D^2 - a^2 - \frac{\omega}{Pr}\right)w - Ra^2\theta - \sqrt{(Ta)}D\zeta = 0 \tag{3}$$

$$(D^2 - a^2 - \omega)\theta + w = 0 \tag{4}$$

and, for the porous layer, are

$$\nabla_m \cdot \mathbf{u}_m = 0 \tag{5}$$

$$-\left(\frac{1}{K} + \frac{\omega_m}{Pr_m}\right)\zeta_m + \sqrt{(Ta_m)}D_m w_m = 0 \tag{6}$$

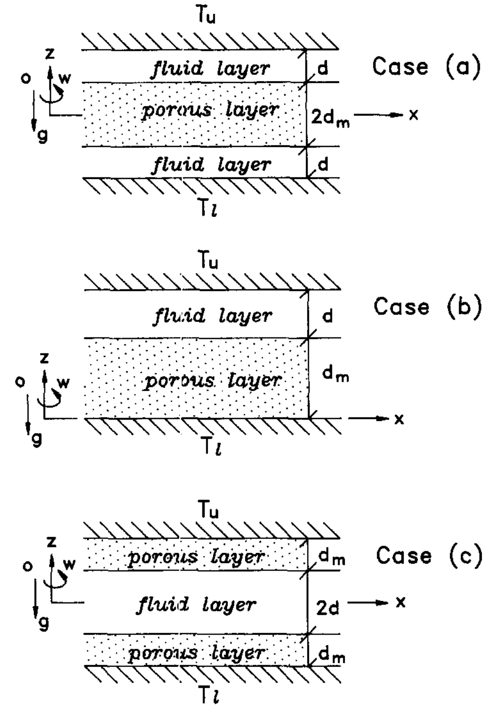

Fig. 1. Physical configuration for cases (a), (b) and (c).

$$-\left(\frac{1}{K}+\frac{\omega_m}{Pr_m}\right)(D_m^2-a_m^2)w_m$$

$$= R_m a_m^2\theta_m+\sqrt{(Ta_m)}D_m\zeta_m \quad (7)$$

$$\left(D_m^2-a_m^2-\frac{\omega_m}{p_e}\right)\theta_m+w_m = 0. \quad (8)$$

The thermal and hydrodynamic conditions at the rigid boundary are

$$\theta = 0 \quad (9)$$

$$w = Dw = \zeta = 0 \quad (10)$$

$$\theta_m = 0 \quad (11)$$

$$w_m = D_m w_m = \zeta_m = 0. \quad (12)$$

At the interface between the fluid and porous layers, the continuity of temperature, heat flux, vertical velocity and normal stress and, as well, the slipping conditions give rise to the interfacial conditions,

$$\theta = \varepsilon_t\theta_m \quad (13)$$

$$D\theta = D_m\theta_m \quad (14)$$

$$\bar{\varepsilon}_t w = w_m \quad (15)$$

$$\left(D^2-3a^2-\frac{\omega}{Pr}\right)Dw-\sqrt{(Ta)}\zeta$$

$$= \frac{-1}{\bar{\varepsilon}_t\hat{d}^3}\left[\left(\frac{1}{K}+\frac{\omega_m}{Pr_m}\right)D_m w_m+\sqrt{(Ta_m)}\zeta_m\right] \quad (16)$$

$$D^2 w = \pm\frac{\tilde{\alpha}}{\hat{d}K^{1/2}}\left(Dw-\frac{1}{\bar{\varepsilon}_t\hat{d}}D_m w_m\right) \quad (17)$$

$$D\zeta = \pm\frac{\tilde{\alpha}}{\hat{d}K^{1/2}}\left(\zeta-\frac{1}{\bar{\varepsilon}_t\hat{d}}\zeta_m\right) \quad (18)$$

where the $-$ sign holds for cases (a) and (b), while the $+$ sign holds for case (c). The slip conditions are originally proposed and experimentally proven valid for unidirectional flow [12, 16] and is modified to include the Coriolis effect.

Either case (a) or (c) can be treated symmetrically by choosing the mid-plane as a symmetrical plane. For case (a), the mid-plane is assumed symmetrically rigid such that the porous layer is separated into upper and lower parts by a thin slab of infinitesimal thickness and boundary conditions become

$$D_m\theta_m = 0 \quad (19)$$

$$D_m w_m = D_m^2 w_m = D_m\zeta_m = 0. \quad (20)$$

For case (c), the mid-plane is assumed symmetrically free and boundary conditions become

$$D\theta = 0 \quad (21)$$

$$Dw = D^3 w = D^2\zeta = 0. \quad (22)$$

The dimensionless physical parameters have the following relations,

$$R_m = \hat{d}^2\varepsilon_t\bar{\varepsilon}_t R$$

$$a_m^2 = \hat{d}^2 a^2$$

$$Ta_m = \hat{d}^4 Ta.$$

NUMERICAL PROCEDURE

The governing equations, which are sets of ordinary differential equations of order eight in the fluid layer and of order four in the porous layer, including equations (1)–(4) and (5)–(8), form a Sturm–Liouville's problem with the Rayleigh number R or R_m as the eigenvalue, while keep other physical parameters $\hat{d}$, ε_t, $\bar{\varepsilon}_t$, K, Ta, Ta_m, a and a_m fixed. The problem is solved by using the Runge–Kutta–Gill's shooting method of order four.

For the fluid layer, we let

$$w = u_1$$

$$Dw = Du_1 = u_2 \quad (23)$$

$$D^2 w = Du_2 = u_3 \quad (24)$$

$$D^3 w = Du_3 = u_4 \quad (25)$$

$$D^4 w = \left(2a^2+\frac{\omega}{Pr}\right)u_3-\left(a^2+\frac{\omega}{Pr}\right)a^2 u_1$$

$$+Ra^2 u_5+\sqrt{(Ta)}u_8 \quad (26)$$

$$\theta = u_5$$

$$D\theta = Du_5 = u_6 \quad (27)$$

$$D^2\theta = (a^2+\omega)u_5 - u_1 \quad (28)$$

$$\zeta = u_7$$

$$D\zeta = Du_7 = u_8 \quad (29)$$

$$D^2\zeta = \left(a^2+\frac{\omega}{Pr}\right)u_7 - \sqrt{(Ta)}u_2 \quad (30)$$

and, for the porous layer, we let

$$w_m = v_1$$

$$D_m w_m = D_m v_1 = v_2 \quad (31)$$

$$D_m^2 w_m = \left[Ta_m + \left(\frac{1}{K}+\frac{\omega_m}{Pr_m}\right)^2\right]^{-1} \times \left[\left(\frac{1}{K}+\frac{\omega_m}{Pr_m}\right)^2 a_m^2 v_1 - \left(\frac{1}{K}+\frac{\omega_m}{Pr_m}\right)R_m a_m^2 v_3\right] \quad (32)$$

$$\theta_m = v_3$$

$$D_m\theta_m = D_m v_3 = v_4 \quad (33)$$

$$D_m^2\theta_m = \left(a_m^2+\frac{\omega_m}{\rho_e}\right)v_3 - v_1. \quad (34)$$

For case (b), the boundary conditions (13)–(18), at the interface $z = 0$ or $z_m = 1$, become

$$u_5 = \varepsilon_t v_3 \quad (35)$$

$$u_6 = v_4 \quad (36)$$

$$u_8 = \frac{\tilde{\alpha}}{\hat{d}K^{1/2}}\left(u_7 - \left(\frac{1}{K}+\frac{\omega_m}{Pr_m}\right)\frac{\hat{d}}{\varepsilon_t}\sqrt{(Ta)}v_2\right) \quad (37)$$

$$u_1 = v_1/\overline{\varepsilon_t} \quad (38)$$

$$u_3 = \frac{\tilde{\alpha}}{\hat{d}K^{1/2}}\left(u_2 - \frac{1}{\overline{\varepsilon_t}\hat{d}}v_2\right) \quad (39)$$

$$u_4 - \left(3a^2+\frac{\omega}{Pr}\right)u_2 - \sqrt{(Ta)}u_7 = \frac{1}{\overline{\varepsilon_t}\hat{d}^3}\left[-\left(\frac{1}{K}+\frac{\omega_m}{Pr_m}\right) - \left(\frac{1}{K}+\frac{\omega_m}{Pr_m}\right)^{-1} Ta_m\right]v_2. \quad (40)$$

At $z = 1$, there are four boundary conditions (9) and (10),

$$u_1 = u_2 = u_5 = u_7 = 0 \quad (41)$$

we shall guess four more boundary conditions by choosing

$$u_3 = b_1 \quad u_4 = b_2 \quad u_6 = b_3 \quad \text{and} \quad u_8 = b_4 \quad (42)$$

then we have

$$\mathbf{U} = b_1\mathbf{U}_1 + b_2\mathbf{U}_2 + b_3\mathbf{U}_3 + b_4\mathbf{U}_4 \quad (43)$$

where

$$\mathbf{U}_1 = [0,0,1,0,0,0,0,0]^T$$
$$\mathbf{U}_2 = [0,0,0,1,0,0,0,0]^T$$
$$\mathbf{U}_3 = [0,0,0,0,0,1,0,0]^T$$
$$\mathbf{U}_4 = [0,0,0,0,0,0,0,1]^T.$$

We may guess a value for R or R_m, assume $\mathbf{U}_i$, $i = 1,4$, as a set of initial conditions and start, using the Runge–Kutta–Gill's shooting method, from $z = 1$ and try to match the interfacial boundary conditions at $z = 0$.

There are two boundary conditions (11) and (12) at $z_m = 0$,

$$v_1 = v_3 = 0. \quad (44)$$

We shall guess two more boundary conditions by choosing

$$v_2 = c_1 \quad \text{and} \quad v_4 = c_2$$

then we have

$$\mathbf{V} = c_1\mathbf{V}_1 + c_2\mathbf{V}_2 \quad (45)$$

where

$$\mathbf{V}_1 = [0,1,0,0]^T$$
$$\mathbf{V}_2 = [0,0,0,1]^T.$$

We use the guessing value of R or R_m, assume $\mathbf{V}_i$, $i = 1,2$, as a set of initial conditions and start, again using the Runge–Kutta–Gill's shooting method, from $z_m = 0$ and try to match the interfacial boundary conditions at $z_m = 1$.

In considering the stationary state only, the boundary conditions at the interface $z = 0$ or $z_m = 1$ turn into a matrix form,

$$\mathbf{MB} = 0$$

where

$$\mathbf{M} = [m_{ij}], \quad i,j = 1,6$$

$$\mathbf{B} = [b_1, b_2, b_3, b_4, -c_1, -c_2]^T$$

$$m_{1i} = \mathbf{U}_i^5, \quad i = 1,4; \quad m_{1j+4} = \varepsilon_t\mathbf{V}_j^3, \quad j = 1,2$$

$$m_{2i} = \mathbf{U}_i^6, \quad i = 1,4; \quad m_{2j+4} = \mathbf{V}_j^4, \quad j = 1,2$$

$$m_{3i} = \mathbf{U}_i^8 - \frac{\tilde{\alpha}}{\hat{d}K^{1/2}}\mathbf{U}_i^7, \quad i = 1,4;$$

$$m_{3j+4} = -\frac{\tilde{\alpha}K^{1/2}}{\overline{\varepsilon_t}}\sqrt{(Ta)}\mathbf{V}_j^2, \quad j = 1,2$$

$$m_{4i} = \mathbf{U}_i^1, \quad i = 1,4; \quad m_{4j+4} = \mathbf{V}_j^1/\varepsilon_t, \quad j = 1,2$$

$$m_{5i} = \mathbf{U}_i^3 - \frac{\tilde{\alpha}}{\hat{d}K^{1/2}}\mathbf{U}_i^2, \quad i = 1,4;$$

$$m_{5j+4} = -\frac{\tilde{\alpha}}{\bar{\varepsilon}_t\hat{d}^2K^{1/2}}\mathbf{V}_j^2, \quad j = 1,2$$

$$m_{6i} = \mathbf{U}_i^4 - 3a^2\mathbf{U}_i^2 - \sqrt{(Ta)}\mathbf{U}_i^7, \quad i = 1,4$$

$$m_{6j+4} = \frac{1}{\bar{\varepsilon}_t\hat{d}^3}\left(-\frac{1}{K} - KTa_m\right)\mathbf{V}_j^2, \quad j = 1,2$$

and $\mathbf{U}_i^k$ is the kth element of $\mathbf{U}_i$ and $\mathbf{V}_j^k$ is the kth element of $\mathbf{V}_j$.

For non-trivial solutions for b_i and c_i, the determinant of matrix $\mathbb{M}$ shall be zero and a newly guessed value of R or R_m is thus obtained. The Rayleigh number R or R_m as a function of a or a_m would give rise to a minimum point, marking the critical state and corresponding to a critical Rayleigh number R_c or R_{mc} and a related critical wavenumber a_c or a_{mc}.

For cases (a) and (c), we adopt the same procedure, except we need to deal with a different set of boundary conditions at the mid-plane as suggested in equations (19)–(22).

RESULTS AND DISCUSSIONS

The general solutions of special cases of $Ta = 0$ have been solved, using the power series method [1, 2, 17]. The ranges of physical parameters $\hat{d}$, ε_t, K, $\tilde{\alpha}$ and Ta are chosen as 10^{-10}–10^{10}, 10^{-3} $\hat{d}$–$10\hat{d}$, 10^{-2}–10^{-10}, 10^{-1}–10 and 0–10^5, respectively. Without loss of generality, we let $\bar{\varepsilon}_t = \varepsilon_t$ for simplicity.

In the limit $\hat{d} \to 0$ or ∞, the slip and thermal boundary conditions, at the interface between the fluid and porous layers, can be successfully reduced to be free, rigid or impermeable and isothermal or with a fixed heat flux. As $\hat{d} \to 0$ and $Ta = 0$, the systems of cases (b) and (c) become single fluid layers of corresponding depths d and $2d$ with upper and lower boundary conditions isothermal and rigid and the critical values [R_c, a_c] are [1707.762, 3.12] and [106.735, 1.56] respectively [14, 17, 18]. The system of case (a) becomes a single fluid layer of depth $2d$ and is separated at the mid-plane of $z = 0$, where the rigid boundary is imposed with a fixed heat flux and the critical value [R_c, a_c] is [1296, 2.56]. Taslim and Narusawa [1] has shown that, for $Ta = 0$, $\tilde{\alpha} = 1$, $\varepsilon_t = 1$, $K = 10^{-10}$ and $\hat{d} = 10^{-2}$, the critical value R_c is 1295.9. Catton and Lienhard [13], replacing the porous layer by a thin solid layer, has shown that the critical value R_c is 1299.8.

As $\hat{d} \to \infty$ and $Ta = 0$, the system becomes a single porous layer of depth $2d_m$ with upper and lower boundaries isothermal and free for case (a) and of depth d_m with the upper boundary isothermal and free and the lower boundary isothermal and impermeable for case (b) and of depth $2d_m$ with upper and lower boundaries isothermal and impermeable and the mid-plane, at $z_m = 1$, symmetrically free for case (c). For porous layers with upper and lower boundaries impermeable, the critical values [R_{mc}, a_{mc}], are [39.4784, 3.1416] for a depth d_m and [9.8696, 1.5708] for a depth $2d_m$ [19] and, for a porous layer with upper and lower boundaries free, the critical value is [9.804, 1.565] for a depth $2d_m$ [2].

Hydrodynamically, the thickness of a fluid or porous layer may act as a dominant effect on determining the onset of thermal instability. A thicker (thinner) layer considered tends to damp out more (less) thermal disturbances and weaken (strengthen) the thermal coupling with its adjacent layer such that it becomes more (less) stabilizing and has a larger (smaller) critical Rayleigh number. It is obvious that the larger the depth ratio $\hat{d}$, the thicker the fluid layer or the thinner the porous layer. Thermodynamically, a stronger thermal interaction between the layers does destabilize an individual layer. The layer with a small conductivity would dissipate less thermal disturbance and weaken the stability of itself or enhance that of the other. The critical Rayleigh number and wavenumber [R_c, a_c] of a single fluid layer with upper and lower boundaries rigid is [1707.762, 3.12] for both boundaries isothermal, [720, 0] for both boundaries with fixed heat flux and [1296, 2.56] for one boundary isothermal and the other one with a fixed heat flux. The fluid layer destabilizes the most for both boundaries with fixed heat flux and the least for both boundaries isothermal. In the limit of the thermal conductivity ratio k/k_m approaching to zero or infinity, the porous layer could be treated as being isothermal or with a fixed heat flux to the fluid layer, respectively. The critical Rayleigh number R_c is expected to decrease with the thermal conductivity ratio k/k_m. Non-slip effects of the rigid or impermeable boundary are stabilizing, while stress-free effects of the free boundary are destabilizing. However, effects of the slip boundary, depending strongly on $\hat{d}$, K and $\tilde{\alpha}$, lie between the two.

The critical values [R_c, a_c] and [R_{mc}, a_{mc}], for various $\hat{d}$, K and Ta, are tabulated for cases (a), (b) and (c) in Table 1, which gives an excellent comparison with the previous works [1, 2], considering $Ta = 0$ and $K \leqslant 10^{-4}$. For smaller values of $\hat{d}$ less than one in all cases, except case (a) with the limit $K \to 0$, the porous layer becomes thicker and acts as a destabilizing factor to the fluid layer hydrodynamically. As $\hat{d}$ increases from zero and up, the fluid layer becomes more destabilizing and the critical Rayleigh number R_c decreases. For case (a) with the limit $K \to 0$, the physical property of the porous layer tends to be more solid-like and the hydrodynamical boundary conditions become less important in destabilizing the system. Due to the symmetrical assumptions, the thermal boundary condition at the mid-plane, varying from an adiabatic one, related to $\hat{d} = 0$ (i.e. $\varepsilon_t = 0$), and transitting to an isothermal one, related to $\hat{d} \gg 0$, prevails on determining the onset of thermal convection. As $\hat{d}$ increases from zero and up, the fluid layer becomes less desta-

Table 1. Effects of K, $\hat{d}$ and Ta on the critical values with $\tilde{\alpha} = 1$ and $\varepsilon_t = 1.0\hat{d}$

	$K = 10^{-4}$, $Ta = 0$						$K = 10^{-4}$, $Ta = 10^3$					
	Case (a)		Case (b)		Case (c)		Case (a)		Case (b)		Case (c)	
$\hat{d}$	R_c	a_c	R_c	a_c	R_c	a_c	R_c	a_c	R_c	a_c	R_c	a_c
0	1296.681	2.552	1709.183	3.117	106.740	1.5582	1720.570	2.928	2152.135	3.485	371.848	2.595
10^{-3}	1297.549	2.553	1707.764	3.116	106.652	1.5577	1721.696	2.929	2150.555	3.484	371.672	2.594
10^{-2}	1305.196	2.555	1695.423	3.107	105.869	1.5531	1731.575	2.933	2136.849	3.474	370.134	2.589
10^{-1}	1367.153	2.558	1604.888	3.027	99.324	1.5100	1808.034	2.990	2038.485	3.392	358.087	2.540
1	1419.579	2.761	1422.058	2.776	78.100	1.2687	1851.363	3.159	1852.693	3.167	329.109	2.361

	$K = 10^{-4}$, $Ta_m = 0$						$K = 10^{-4}$, $Ta_m = 10^3$					
	Case (a)		Case (b)		Case (c)		Case (a)		Case (b)		Case (c)	
$\hat{d}$	$R_{mc}*K$	a_{mc}	$R_{mc}*K$	a_{mc}	$R_{mc}*K$	a_{mc}	$R_{mc}*K$	a_{mc}	$R_{mc}*K$	a_{mc}	$R_{mc}*K$	a_{mc}
10	5.3099	1.094	24.2750	2.414	7.2098	1.526	5.3118	1.095	24.2789	2.414	7.2101	1.526
10^2	9.7277	1.559	38.9179	3.119	9.5787	1.563	9.7278	1.559	38.9181	3.119	9.5788	1.563
10^3	9.8594	1.570	39.4433	3.140	9.8401	1.570	9.8594	1.570	39.4435	3.140	9.8402	1.570
∞	9.8697	1.571	39.4846	3.142	9.8697	1.571	9.8698	1.571	39.4848	3.142	9.8698	1.571

	$K = 10^{-2}$, $Ta = 0$						$K = 10^{-2}$, $Ta = 10^3$					
	Case (a)		Case (b)		Case (c)		Case (a)		Case (b)		Case (c)	
$\hat{d}$	R_c	a_c	R_c	a_c	R_c	a_c	R_c	a_c	R_c	a_c	R_c	a_c
0	1296.681	2.552	1709.183	3.117	106.740	1.558	1720.570	2.928	2152.135	3.485	371.848	2.595
10^{-3}	1296.506	2.551	1707.271	3.116	106.621	1.558	1720.446	2.927	2150.063	3.484	371.623	2.594
10^{-2}	1294.663	2.542	1690.482	3.105	105.563	1.552	1718.955	2.919	2131.904	3.473	369.635	2.589
10^{-1}	1251.825	2.432	1552.770	3.008	96.359	1.501	1670.871	2.800	1983.731	3.381	352.436	2.537
1	1229.646	2.224	465.718	1.799	43.726	1.142	1500.111	2.500	670.691	2.156	124.724	1.344

	$K = 10^{-2}$, $Ta_m = 0$						$K = 10^{-2}$, $Ta_m = 10^3$					
	Case (a)		Case (b)		Case (c)		Case (a)		Case (b)		Case (c)	
$\hat{d}$	$R_{mc}*K$	a_{mc}	$R_{mc}*K$	a_{mc}	$R_{mc}*K$	a_{mc}	$R_{mc}*K$	a_{mc}	$R_{mc}*K$	a_{mc}	$R_{mc}*K$	a_{mc}
10	8.6089	1.464	34.6326	2.927	7.3795	1.506	9.0341	1.499	36.3441	2.995	7.7653	1.542
10^2	9.7682	1.563	39.0831	3.126	9.5808	1.563	10.2531	1.600	41.0231	3.201	10.0566	1.600
10^3	9.8598	1.570	39.4450	3.140	9.8404	1.570	10.3472	1.608	41.3948	3.216	10.3268	1.608
∞	9.8697	1.571	39.4846	3.142	9.8697	1.571	10.3573	1.609	41.4353	3.218	10.3573	1.609

bilizing instead and the critical Rayleigh number R_c increases. As $\hat{d}$ approaches a unit, the physical models of cases (a) and (b) become asymptotical to each other and the critical Rayleigh numbers for both cases are approximately equal. For larger values of $\hat{d}$ greater than ten, the fluid layer would become a destabilizing factor with respect to the porous layer instead. As $\hat{d}$ increases from a large value to infinity, the fluid layer, would become thinner and acts as a less destabilizing factor to the porous layer and the critical Rayleigh number R_{mc} is expected to increase. As $\hat{d}$ approaches infinity, the physical models of cases (a), (b) and (c) become asymptotical to one another, irrespective of the values of K and Ta, except case (b) possesses a depth of twice the thickness. From the above results, the effect of rotation on the flow is insignificant in a porous medium of small permeability. Critical values $[R_c, a_c]$ as functions of $\hat{d}$ for various K and Ta are plotted in Fig. 2 for cases (a) and (b) and in Fig. 3 for case (c), respectively. The fluid-limits of $\hat{d} \to 0$ and the porous limits of $\hat{d} \to \infty$ are obvious, as shown in Fig. 3. Rapid variations of the critical values $[R_c, a_c]$ with $\hat{d}$ occur when $0.1 < \hat{d} < 10$, in which range the occurrence of onset of thermal convection is being transitted from the fluid layer type to the porous one and has been studied for $Ta = 0$ [1].

As $\tilde{\alpha}$ increases or K decreases, the interface and the porous layer, tending to be more solid-like, would make the system become less destabilizing and the critical Rayleigh number R_c is expected to increase. The critical values $[R_c, a_c]$, for various $\tilde{\alpha}$, K, ε_t and Ta, are tabulated in Table 2 and, as functions of K for various $\tilde{\alpha}$ and Ta, are shown in Fig. 4 for case (a). It shows that, for $K \leqslant 10^{-6}$ and $Ta = 0$, variations of the critical Rayleigh number R_c with K and $\tilde{\alpha}$ are insignificant and a solid limit, as $K \to 0$, is obtained.

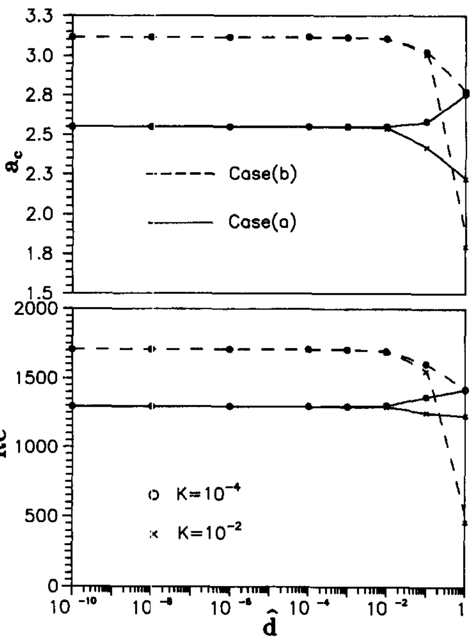

Fig. 2. Variations of critical conditions (R_c, a_c) with $\hat{d}$ for cases (a) and (b) with $Ta = 0$, $\tilde{\alpha} = 1$ and $\varepsilon_t = \hat{d}$.

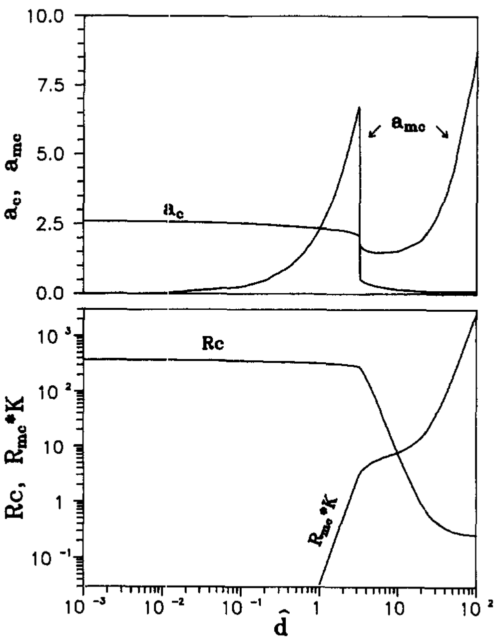

Fig. 3. Variations of critical conditions (R_c, a_c) with $\hat{d}$ for case (c) with $Ta = 10^3$, $K = 10^{-4}$, $\tilde{\alpha} = 1$ and $\varepsilon_t = \hat{d}$.

For $10^{-6} < K < 10^{-4}$ and $Ta = 0$, variations of the critical Rayleigh number R_c with $\tilde{\alpha}$ are not obvious, when $1 \leqslant \tilde{\alpha} \leqslant 10$. The combined effects of a smaller $\tilde{\alpha}$ and a larger K give rise to a more destabilizing state to the fluid layer and thus a decreasing critical Rayleigh number. Variations of the critical wavenumber a_c with either K or $\tilde{\alpha}$ are insensitively decreasing as well for $K < 10^{-4}$. Also from Fig. 2, variations of the critical Rayleigh number R_c with the permeability K are negligible for $\hat{d} < 10^{-4}$ and irrespective of Ta. However, for $\hat{d} > 10^{-2}$, case (b) shows the most obvious variation of all.

The physical parameter ε_t is related to the depth ratio $\hat{d}$ and the conductivity ratio k/k_m. For $k/k_m = 1$ and $\varepsilon_t = \hat{d}$, the sole effect of the depth ratio $\hat{d}$ has been discussed previously. We would merely concentrate on the effect of thermal conductivity ratio k/k_m. Figure 5 shows, for case (b), the variations of the critical value $[R_c, a_c]$ with K, for various values of ε_t and Ta. For $\hat{d} = 1$ and $\varepsilon_t \to 0$, the porous layer is assumed to be perfectly conductive and the interfacial condition is isothermal. As ε_t is increased, the thermal interaction between the fluid and porous layers, due to a more destabilizing temperature profile, is enhanced and the critical Rayleigh number R_c decreases. As $\varepsilon_t \to \infty$, the porous layer is assumed to be perfectly adiabatic and the interface is subject to a fixed heat flux. The critical values $[R_c, a_c]$ for case (c) are tabulated, for various values of $\hat{d}$, k/k_m and ε_t, in Table 3, which is compared very well within a small relative error with the previous works [1, 13], and plotted, as functions of ε_t for various values of $\tilde{\alpha}$ and Ta, in Fig. 6. Significant variations of the critical values $[R_c, a_c]$ with ε_t, for $1 < \varepsilon_t < 10$, and with $\tilde{\alpha}$, for $0.1 < \tilde{\alpha} < 1$, do occur. For $\hat{d} = 1$, Fig. 6 shows the limiting values of the critical Rayleigh number R_c for both cases of isothermal condition and constant heat flux condition at the interface. For varying $\hat{d}$, Table 3 still illustrates this kind of trend, especially when the conductivity ratio k/k_m becomes large. A similar discussion with the relation $R_c/R_{mc} = 1/\varepsilon_t^2\hat{d}^2$ would conclude that the critical Rayleigh number R_{mc} increases as ε_t is increased.

Taylor–Proudman theorem predicts that all steady slow motions of inviscid flows in a rotating system are necessarily two-dimensional [14]. The sole effect of rotation suppresses the onset of thermal convection and raise the stability of the system, the critical Rayleigh numbers R_c and R_{mc} are expected to increase with Taylor number Ta. Figures 4–8 have shown such trends.

In the limit $\hat{d} \to 0$ or ∞ and $Ta = 10^3$, the system may become a single fluid layer of depth d with the critical value $[R_c, a_c]$ being [2151.7, 3.50] [14] or a single porous layer of depth d_m with the critical value $[R_{mc}, a_{mc}]$ being [40.08, 3.20] for $K = 10^{-4}$ [15], which case does include an extra viscous shear term.

Variations of the critical values $[R_c, a_c]$ with Ta, for various values of $\hat{d}$ and $K = 10^{-4}$ and $\tilde{\alpha} = 1$ are plotted in Fig. 7 for case (b). The critical values $[R_c, a_c]$, for $\hat{d} \leqslant 1$, increases with Ta slowly for $Ta < 10^2$ and rapidly for $Ta > 10^3$. As the Taylor number Ta goes far beyond 10^4, this increasing trend becomes irrespective of the depth ratio $\hat{d}$.

Variations of the critical values $[R_c, a_c]$ with Ta, for various K and $\hat{d} = 1$, are plotted in Fig. 8 for case (c). The critical values $[R_c, a_c]$, strongly affected by Taylor number Ta when $Ta > 10^2$, increase with Ta slightly for $K > 10^{-4}$, in which range the porous layer tends to be more fluid-like, and significantly for $K < 10^{-4}$,

Table 2. Effects of $\tilde{\alpha}$, ε_t and K on the critical values with $\hat{d} = 1.0$

R_c [a_c]		$Ta = 0$					
		Case (a)		Case (b)		Case (c)	
$\tilde{\alpha}$	ε_t	$K = 10^{-4}$	$K = 10^{-10}$	$K = 10^{-4}$	$K = 10^{-10}$	$K = 10^{-4}$	$K = 10^{-10}$
0.1	1	1171.3471	1492.4444	1174.5685	1493.9439	61.1855	81.3471
		[2.601]	[2.810]	[2.622]	[2.819]	[1.197]	[1.280]
1	0.1	1606.9933	1669.1169	1607.4334	1669.4333	98.6608	102.1779
		[3.034]	[3.061]	[3.037]	[3.063]	[1.503]	[1.514]
	1	1419.5799	1492.9826	1422.0583	1494.4811	78.1005	81.4655
		[2.761]	[2.811]	[2.776]	[2.820]	[1.269]	[1.280]
	10	222.3201	1330.0916	1150.5234	1330.7879	53.7797	57.3160
		[0.215]	[2.592]	[2.300]	[2.597]	[0.830]	[0.844]
10	1	1467.1606	1493.0365	1469.5411	1494.5349	80.7437	81.4683
		[2.785]	[2.811]	[2.799]	[2.820]	[1.278]	[1.280]

R_c [a_c]		$Ta = 10^3$					
		Case (a)		Case (b)		Case (c)	
$\tilde{\alpha}$	ε_t	$K = 10^{-4}$	$K = 10^{-10}$	$K = 10^{-4}$	$K = 10^{-10}$	$K = 10^{-4}$	$K = 10^{-10}$
0.1	1	1649.9332	1931.8536	1651.4188	1932.5689	320.8990	338.1897
		[3.100]	[3.204]	[3.109]	[3.208]	[2.430]	[2.383]
1	0.1	2045.7903	2112.0399	2046.0205	2112.1908	358.1496	365.9085
		[3.415]	[3.435]	[3.416]	[3.436]	[2.551]	[2.562]
	1	1851.3631	1932.4048	1852.6932	1933.1198	329.1095	338.2444
		[3.159]	[3.204]	[3.167]	[3.208]	[2.361]	[2.383]
	10	247.5715	1757.8829	2793.4069	1758.2407	289.1366	307.6543
		[0.383]	[2.975]	[2.684]	[2.978]	[1.904]	[2.097]
10	1	1898.5318	1932.4600	1899.8244	1933.1749	333.5916	338.2498
		[3.174]	[3.204]	[3.182]	[3.208]	[2.363]	[2.383]

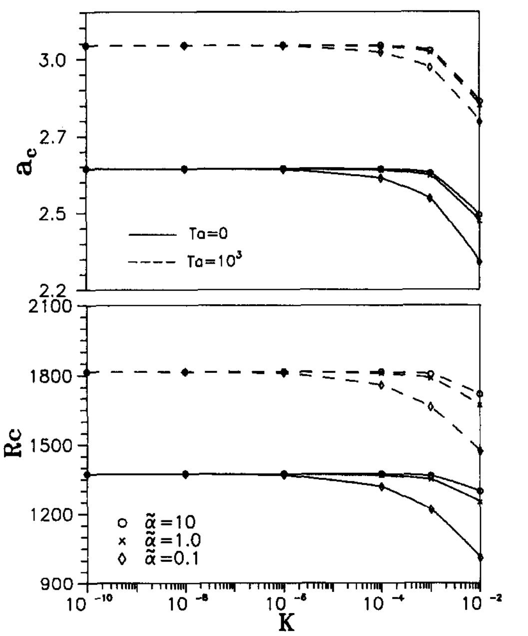

Fig. 4. Variations of critical conditions (R_c, a_c) with K for case (a) with $\varepsilon_t = \hat{d} = 0.1$.

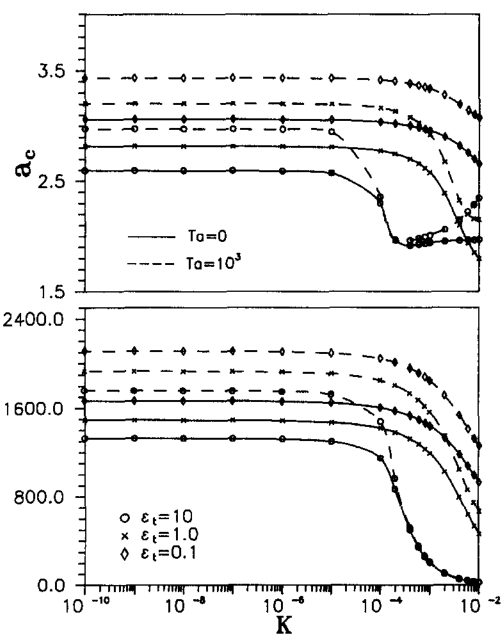

Fig. 5. Variations of critical conditions (R_c, a_c) with K for case (b) with $\hat{d} = 1$ and $\tilde{\alpha} = 1$.

in which the porous layer tends to be more solid-like. Figure 5 does depict such a result, especially for large values of ε_t.

While the critical values [R_{mc}, a_{mc}] increase very insensitively with Ta for $\hat{d} > 10$, as shown in Table 1. Effects of Ta on the onset of thermal instability inside a porous layer become less important.

Critical values [R_c, a_c] and [R_{mc}, a_{mc}] as functions of $\hat{d}$, for $Ta = 10^3$, are plotted in Fig. 3 for case (c). The fluid-limits of $\hat{d} \rightarrow 0$ and the porous limits of $\hat{d} \rightarrow \infty$

Table 3. Comparison of results of this study with previous works for case (a) with $\tilde{\alpha} = 1.0$, $K = 10^{-10}$ and $\varepsilon_t = (k/k_m)\hat{d}$

		$Ta = 0$	k/k_m 0.2	1.0	5.0	100
	0.01	Catton–Lienhard	1345.3	1312.6	1305.4	1299.8
		Taslim–Narusawa	1338.4	1304.9	1297.6	1295.9
		This study	1339.5	1305.9	1298.5	1296.8
$\hat{d}$	0.1	Catton–Lienhard	1527.9	1378.5	1318.4	1297.5
		Taslim–Narusawa	1525.7	1372.9	1313.4	1296.7
		This study	1526.9	1373.9	1314.3	1297.6
	1.0	Catton–Lienhard	1634.9	1492.2	1358.2	1299.6
		Taslim–Narusawa	1634.6	1491.8	1357.8	1299.3
		This study	1635.9	1492.9	1358.8	1300.2

		$Ta = 10^3$	k/k_m 0.2	1.0	5.0	100
	0.01	This study	1774.269	1732.296	1722.959	1720.691
			[2.9585]	[2.9337]	[2.9293]	[2.9283]
$\hat{d}$	0.1	This study	1980.793	1815.285	1742.889	1721.690
			[3.2014]	[2.9945]	[2.9401]	[2.9288]
	1.0	This study	2078.660	1932.405	1789.501	1724.543
			[3.3933]	[3.2038]	[3.0160]	[2.9333]

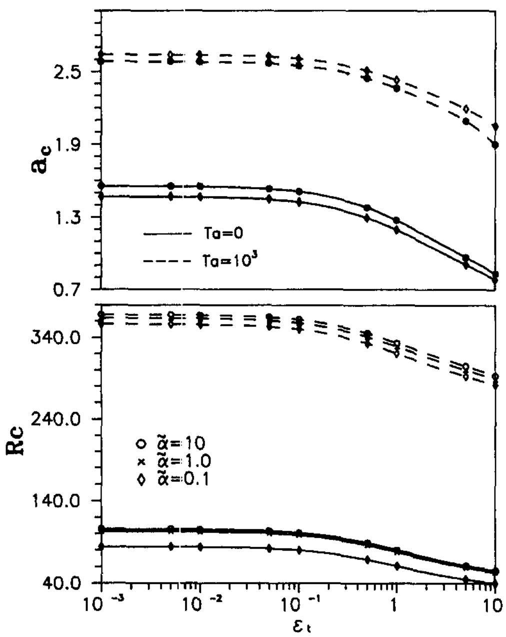

Fig. 6. Variations of critical conditions (R_c, a_c) with ε_t for case (c) with $K = 10^{-4}$ and $\hat{d} = 1$.

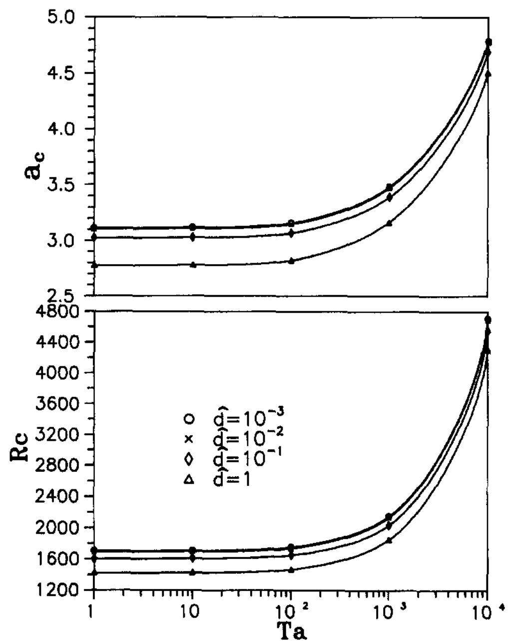

Fig. 7. Variations of critical conditions (R_c, a_c) with Ta for case (b) with $K = 10^{-4}$, $\tilde{\alpha} = 1$ and $\varepsilon_t = \hat{d}$.

are obvious. Rapid variations of the critical values $[R_c, a_c]$ or $[R_{mc}, a_{mc}]$ with $\hat{d}$ occur when $0.1 < \hat{d} < 10$, in which range the occurrence of onset of thermal convection is being transitted from the fluid layer type to the porous one and this case has been studied for $Ta = 0$ [1]. Table 4 shows that this kind of transition, when $Ta = 10^3$, occurs at $\hat{d} = 3.2$, at which depth ratio the onset of thermal instabilities could take place inside both fluid and porous layers.

CONCLUSION

The onset of thermal stabilities of the horizontally superposed systems of fluid and porous layers, in a rotating coordinate, is investigated. The Runge–Kutta–Gill's shooting method, which can be easily modified to solve general problems, is adopted and the results are compared very well with previous works, using the power method. The main conclusions are:

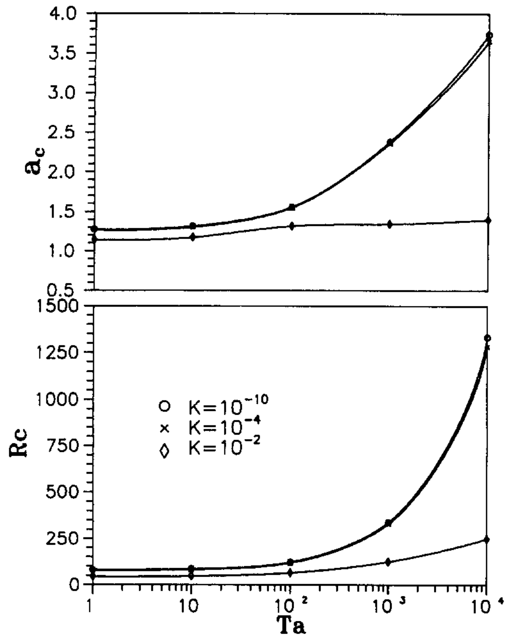

Fig. 8. Variations of critical conditions (R_c, a_c) with Ta for case (c) with $\tilde{\alpha} = 1$ and $\varepsilon_t = \hat{d} = 1$.

Table 4. Variation of critical values with $\hat{d}$ for case (c) with $Ta = 10^3$, $K = 10^{-4}$, $\tilde{\alpha} = 1.0$ and $\varepsilon_t = 1.0\hat{d}$

$\hat{d}$	R_c	a_c	$\hat{d}$	$R_{mc}*K$	a_{mc}
10^{-2}	370.134	[2.589]	3.2	3.011	[6.735]
10^{-1}	358.087	[2.540]	5.0	5.410	[1.503]
1.0	329.109	[2.361]	10	7.759	[1.545]
2.0	313.310	[2.282]	20	14.706	[1.949]
3.2	287.123	[2.105]	30	36.674	[2.685]

(1) For a smaller value of $\hat{d}$, except case (a) with the limit $K \to 0$, the porous layer becomes a destabilizing factor to the fluid layer hydrodynamically. As $\hat{d}$ increases, the critical value R_c decreases. For case (a) with the limit $K \to 0$, the effects of thermal boundary conditions are dominant on determining the onset of thermal convection and critical value R_c increases instead. For a larger value of $\hat{d}$, the fluid layer becomes a destabilizing factor to the porous layer and the critical value R_{mc} increases with the depth ratio $\hat{d}$.

(2) As $\tilde{\alpha}$ increases or K decreases, the slip boundary condition and the porous layer, deviating themselves from the free ones, would make the system become less destabilizing. For $K \geqslant 10^{-6}$ and $Ta = 0$, variations of the critical Rayleigh number R_c with $\tilde{\alpha}$ are not obvious for $1 \leqslant \tilde{\alpha} \leqslant 10$.

(3) For fixed values of $\hat{d}$, as $\varepsilon_t \to 0$, the porous layer is assumed to be perfectly conductive and the interfacial condition is isothermal. As ε_t is increased, the thermal interaction between the fluid and porous layers, due to a more destabilizing temperature profile, is enhanced and the critical Rayleigh number R_c decreases. As $\varepsilon_t \to \infty$, the porous layer is assumed to be perfectly adiabatic and the interface is subject to a fixed heat flux. Significant variations of the critical values [R_c, a_c], for case (c), with ε_t for $1 < \varepsilon_t < 10$, and with $\tilde{\alpha}$, for $0.1 < \tilde{\alpha} < 1$, do occur.

(4) The Taylor–Proudman theorem predicts that all steady slow motions of inviscid flows in a rotating system are necessarily 2D. The sole effect of rotation suppresses the onset of thermal convection and raises the stability of the system, the critical Rayleigh numbers R_c and R_{mc} are expected to increase with Taylor number Ta.

Acknowledgements—The present research was conducted under support (NSC-81-0208-035-03) from the National Science Committee, Taiwan, R.O.C.

REFERENCES

1. M. E. Taslim and U. Narusawa, Thermal stability of horizontally superposed porous and fluid layers, *J. Heat Transfer* **111,** 357–362 (1989).
2. G. Pillatsis, M. E. Taslim and U. Narusawa, Thermal instability of a fluid-saturated porous medium bounded by thin fluid layers, *J. Heat Transfer* **109,** 677–682 (1987).
3. D. A. Nield, Onset of convection in a fluid layer overlying a layer of porous medium, *J. Fluid Mech.* **81,** 513–522 (1977).
4. D. A. Nield, Boundary correction for the Rayleigh–Darcy problem: limitation of the Brinkman equation, *J. Fluid Mech.* **128,** 37–46 (1983).
5. D. Poulikakos, A. Bejan, B. Selimos and K. R. Blake, High Rayleigh number convection in a fluid overlying a porous bed, *Int. J. Heat Fluid Flow* **7,** 109–114 (1986).
6. D. E. Loper and P. H. Roberts, On the motion of an iron-alloy containing a slurry—II. A simple model, *Geophys. Astrophys. Fluid Dyn.* **16,** 83–127 (1980).
7. M. E. Glicksman, S. R. Coriell and G. B. McFadden, Interaction of flow with the crystal–melt interface, *Ann. Rev. Fluid Mech.* **18,** 307–335 (1986).
8. K. Vafai and C. L. Tien, Boundary and inertia effects on flow and heat transfer in porous medium, *Int. J. Heat Mass Transfer* **24,** 195–203 (1981).
9. C. W. Somerton and I. Catton, On the thermal instability of superposed porous and fluid layer, *J. Heat Transfer* **104,** 160–165 (1982).
10. M. Kaviany, Thermal convective instabilities in a porous medium, *J. Heat Transfer* **106,** 137–142 (1984).
11. C. Beckerman, S. Ramadhani and R. Viskanta, Natural convection flow and heat transfer between a fluid layer and a porous layer inside a rectangular enclosure, *AIAA/ASME 4th Thermophysics and Heat Transfer Conference*, Boston, MA, ASME HTD-Vol. 56, pp. 1–12 (1986).
12. G. S. Beavers and D. D. Joseph, Boundary condition at a naturally permeable wall, *J. Fluid Mech.* **30,** 197–207 (1967).
13. I. Catton and J. H. V. Lienhard, Thermal stability of two fluid layers separated by a solid interlayer of finite thickness and thermal conductivity, *J. Heat Transfer* **106,** 605–612 (1984).
14. S. Chandrasekhar, *Hydrodynamic and Hydromagnetic Stability*. Oxford University Press, London (1961).
15. J. J. Jou and J. S. Liaw, Transient thermal convection in a rotation porous medium confined between two rigid

boundaries, *Int. Commun. Heat Mass Transfer* **14**(2), 147–153 (1987).
16. G. S. Beavers, E. M. Sparrow and R. A. Magnuson, Experiments on couples parallel flows in a channel and a bounding porous medium, *J. Basic Engng* **92**, 843–848 (1970).
17. E. M. Sparrow, R. J. Goldstein and V. K. Jonsson, Thermal instability in a horizontal fluid layer: effect of boundary conditions and non-linear temperature profile, *J. Fluid Mech.* **18**, 513–528 (1964).
18. D. A. Nield, The thermohaline Rayleigh–Jeffreys problem, *J. Fluid Mech.* **29**, 545–558 (1967).
19. D. A. Nield, Onset of thermohaline convection in a porous medium, *Water Resour. Res.* **4**, 553–560 (1968).